Available online at www.sciencedirect.com
ScienceDirect
Engineering Geology 89 (2007) 47–66
ENGINEERING GEOLOGY
www.elsevier.com/locate/enggeo

Logistic Regression analysis in the evaluation of mass movements susceptibility: The Aspromonte case study, Calabria, Italy

R. Greco, M. Sorriso-Valvo *, E. Catalano

Consiglio Nazionale delle Ricerche-Istituto di Ricerca per la Protezione idrogeologica, Italy

Received 9 February 2006; received in revised form 8 September 2006; accepted 11 September 2006
Available online 30 October 2006

Abstract

This work describes the application of Logistic Regression (LR) to an assessment of susceptibility to mass movements in a 850 km^2 study area mainly on the Ionian side of the Aspromonte Range, in southern Calabria.

LR is a multivariate function that can be utilised, on the basis of a given set of variables, to calculate the probability that a particular phenomenon (for instance, a landslide) is present. In the present study the set of relevant variables includes: rock type, land use, elevation, slope angle, aspect, slope profile curvature down-slope and across-slope.

The aim of this paper is to evaluate the LR performance when the procedure is based on the surveying of mass movements in part of the study area. The procedure adopted was GIS-based, with a 10 m DEM square-grid; for slope and curvature calculation, four adjacent cells were grouped to form a nine-point set for mathematical processing.

The LR application consists of four steps: sampling, where all relevant characteristics in a part of the area (ca. 27% of the study zone) are assessed; variable parameterisation, where non-parametric variables are transformed into parametric (or semi-parametric) variables (on at least rank scale); model fitting, where regression coefficients are iteratively calculated in the sample area; model application, where the best-fit regression function is applied to the entire study area. This procedure was applied in two ways: first considering all types, then a single type of mass movement.

The ground characteristics of the whole study zone were determined. The LR procedure was first tested by extending the sampling and reclassification steps to the whole study zone to find out the best possible fitting regression; the results of this were then compared with ground truth to maximise performance. Afterwards, the results of LR analysis, based on extension of regression formulas obtained also using 40% sampling zones, were compared with those of the best possible one and ground truth. Comparisons were performed by means of a confusion matrix and a simple correlation between expected vs. observed values for grouped variables. The overall results seem promising: for example, if the 27% sample areas are adopted, 94% of the cells where the probability of the existence of any kind of mass movements is between 85.5% and 95%, are actually affected by mass movements. Results are instead less good when attempting to distinguish between types of mass movement.

Keywords: Mass movements susceptibility; Logistic Regression analysis (LR); GIS, Calabria

1. Introduction

The evaluation of susceptibility to mass movements is the first step towards landslide risk evaluation. It is the foundation upon which all the subsequent procedure rests. It is not an easy task to select the relevant variables and

* Corresponding author. Tel.: +39 0984 835483; fax: +39 0984 835481.
E-mail address: marino.sorriso@irpi.cnr.it (M. Sorriso-Valvo).

0013-7952/$ - see front matter © 2006 Elsevier B.V. All rights reserved.
doi:10.1016/j.enggeo.2006.09.006

evaluate their role correctly but several attempts have been made to minimise subjectivity and error (Brabb et al., 1978; DeGraff and Romesburg, 1980; Brabb, 1982, 1984; Guzzetti and Cardinali, 1989; Maharaj, 1993; Atkinson and Massari, 1998; Fernandez et al., 1999; Ordan et al., 2000; Baeza and Corominas, 2001; Suzen and Doyuran, 2004). The crucial problem remains that, although both simplicity and reliability are necessary, the level of information must be detailed enough to ensure that landslide management is soundly based.

An important step forward was made in the early 1970s with the introduction of GIS to land classification (Carrara et al., 1977, 1978, 1991; Van Westen, 1992; Reichenbach et al., 1993; Carrara and Guzzetti, 1995; Chung et al., 1995; Carrara et al., 1995, 1999; Fernandez et al., 1999; Guzzetti et al., 1999; Lineback et al., 2001; Suzen and Doyuran, 2004).

The recent and rapid development of computing capacity has also allowed scientists to treat large sets of data, a crucial factor when multivariate statistical analysis is used.

Multivariate procedures have long been employed for landslide studies (Carrara et al., 1977, Reger, 1979; Carrara, 1983; Carrara, 1983; Guzzetti et al., 1987; Carrara, 1989; Carrara et al., 1990, 1991, 1992; Guzzetti, 1993; Carrara and Guzzetti, 1995; Chung et al., 1995; Guzzetti et al., 1999; Baeza and Corominas, 2001). Amongst the various evaluation functions, Logistic Regression analysis (LR) presents certain advantages (Berrnknopf et al., 1988; Gorsevski et al., 2000; Dai and Lee, 2002; Ohlmacher and Davis, 2003; Ayalew and Yamagishi, 2004). With this analysis, the spatial probability of the presence of a given event (landslide) in a particular area is assessed, on the basis

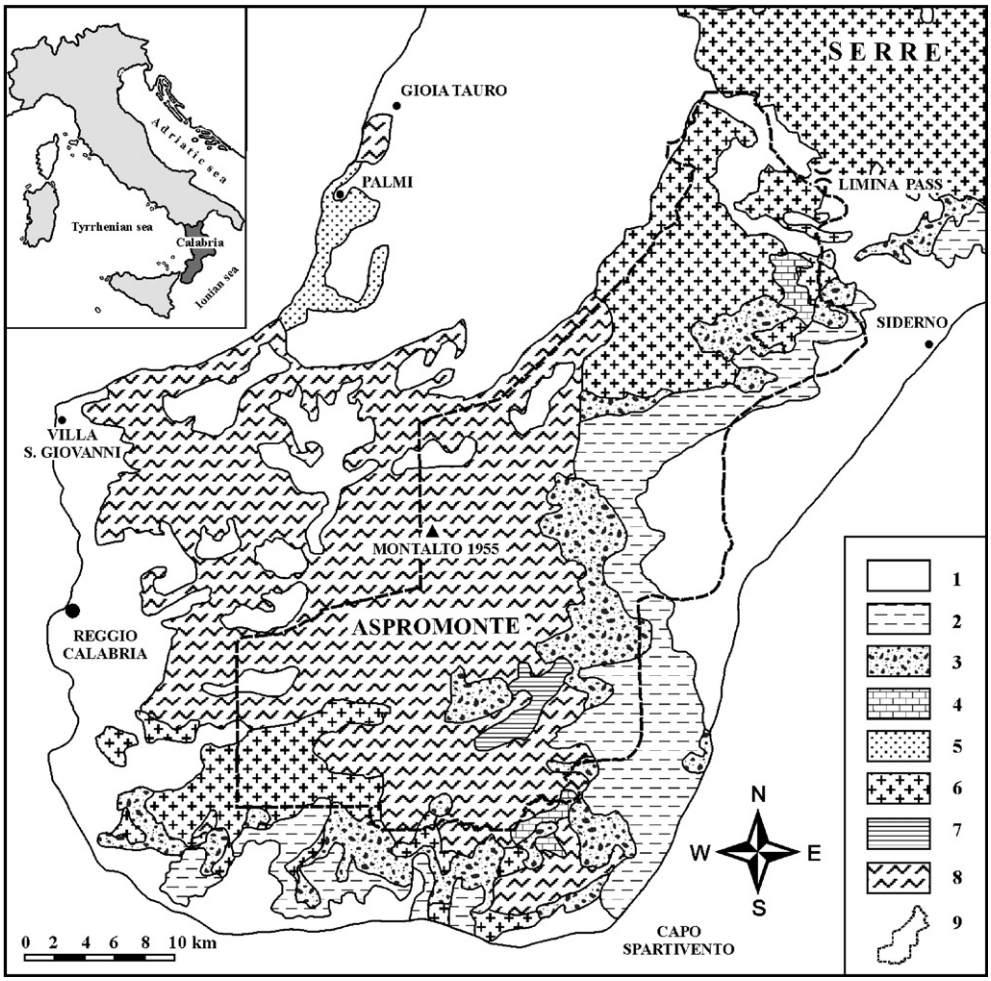

Fig. 1. Geological sketch of Aspromonte massif (from Bonardi et al., 1979, modified). Key to the symbols: 1 = Lower Miocene–Holocene detrital deposits; 2 = *Argille Varicolori* formation; 3 = *Stilo Capo d'Orlando* formation; 4 = *Stilo* and *Aspromonte* units sedimentary cover; 5 = *Palmi-Bagnara* migmatites; 6 = *Stilo* unit; 7 = *Africo* and *Cardeto* units; 8 = *Aspromonte* unit; 9 = study area. In the inset: Italy, with Calabria region (gray).

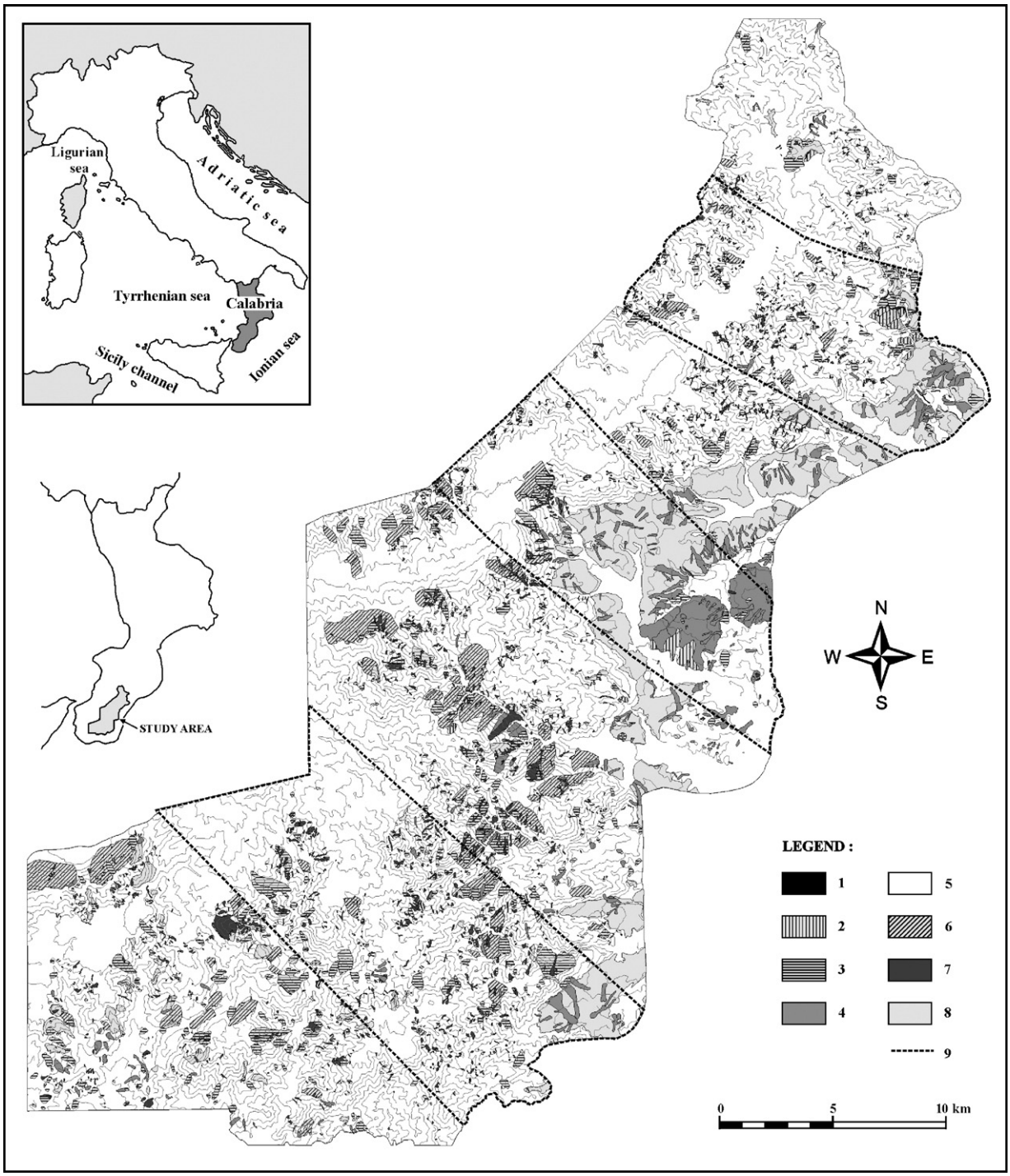

Fig. 2. Slope instability map of the study area. Key to the symbols: 1 = fall/topple; 2 = block slide; 3 = slide; 4 = slide/flow and flow; 5 = lateral spreading; 6 = Sackung; 7 = debris avalanche; 8 = landslide zone; 9 = sampling zones (40%).

of a set of variables. The landslide is thus considered as a dichotomic dependent variable and the probability that its value is 1 is determined. The advantage is that unrealistic negative values of probability, that can occur with other statistical procedures, are not possible with this function (Berrnknopf et al., 1988).

The Logistic Regression (LR) function is:

$$P(y) = \frac{1}{1 + \exp\left(-\sum_{i=1}^{n} a_i X_i\right)} \quad (1)$$

where $P(y)$ is the probability of the existence of the dependent variable; a_i are regression coefficients, i.e. variables weights; X_i are independent variables.

LR is quite robust as concerns the frequency distribution of independent variables, but these cannot be correlated with each other.

There are several ways to use LR for the susceptibility to mass movements assessment (Dai and Lee, 2002; Ohlmacher and Davis, 2003; Ayalew and Yamagishi, 2004). In this paper the authors propose a "sampling procedure", based on four steps: sampling, variable parameterisation, model fitting and model application (see Section 3). The procedure is first performed on a sample zone representative of the whole study area, and then extended to the whole area.

The aim of this work is to estimate the applicability of LR, limiting data collection on landslides only to a part of the study area (the sampling zones). In order to assess the performance of LR, however, the mass movements of the whole study area had to be surveyed.

This sampling procedure has obtained promising results that can reduce costs as well as produce reliable results for regional-scale assessment.

The performance capability of LR analysis used in the sampling procedure can be simply evaluated by means of a confusion matrix and a correlation analysis between estimated values of $P(y)$ and ground frequency of mass movements in each class of probability cells.

The study in Southern Calabria (Italy) was performed over a territory of approximately 850 km^2 which was represented by means of a square-grid cell-based GIS.

2. The case study

2.1. The study area

The study area of 850 km^2 includes most of the Aspromonte range in southern Calabria, in particular the Ionian side and part of its piedmont area (Fig. 1).

The Aspromonte range is a Plio-Pleistocene horst stretching from the Limina Pass in a NE–SW direction; its peak is mount Montalto that reaches 1955 m in elevation. Tectonic uplift has been accelerating since the end of Lower Pleistocene, at an average rate of no more than 1.2 mm/year (Sorriso-Valvo, 1993).

Geologically the study area (Fig. 1) consists of crystalline allochtonous terranes, piled-up in Alpine Orogeny during Eocene–Miocene, partially covered by sin- and post-orogenic transport sedimentary rocks of various composition, including flysch-like conglomerates and sands, clays, marls, evaporites, sands and sandstones, conglomerates, to end with Holocene continental alluvial and thick coastal detrital deposits (Ogniben, 1960; Bonardi et al., 1979). Tectonics and weathering have affected all terranes with growing intensity over time (Carrara et al., 1982; Sorriso-Valvo, 1993).

The climate of the study area is Mediterranean with montane modifications (wetter summers and colder winters, with more than 1 month of snow cover), orographic control on precipitation, and very aggressive characteristics (maximum daily rain up to 125 mm, Versace et al., 1989).

2.2. Data collection

A great deal of data has been collected from published maps (Burton, 1971; APAT, 2005; Sorriso-Valvo, 1982, 2002) and the maps used as data source by Sorriso-Valvo (1979) and Carrara et al. (1982). In order to obtain a homogeneous and updated map of mass movements, detailed aerial photos interpretation and a field survey has been carried out.

The data set also includes lithology, geological structures, morphometry (as DTM-derived maps: slope angle, aspect, across-slope and down slope curvature), and land use. The factors relevant to mass movements were selected on the basis of previous works conducted on part of the study area (ca 120 km^2, cf. Sorriso-Valvo, 1979; Carrara et al., 1982). Structural elements of no relevance in Carrara et al. (1982), were here tentatively reintroduced (presence of fault and distance from fault).

Emi-matrix correlation of all independent variables shows that r is always lower than 0.3, except for elevation and lithology for which $r=0.56$ ($R^2=0.31$), demonstrating that the selected independent variables are valid (Greco, 2004).

2.2.1. Mass movements

LR estimates mass movements probability either outside or inside affected areas, which are used to validate the procedure. Thus, for validating the sample procedure here proposed, the interpretation of the 1954 and 1991 aerial photos (1:33,000 scale) and the field survey were integrated to obtain a 1:10,000 scale map of mass movements phenomena in the whole area. Two sets of aerial photos were used because some phenomena were easier to detect in one set, and other phenomena in the other.

There is no data regarding the activity of mass movements, as the aim of this map is to define their presence or absence. The various types of mass movements were identified using the Varnes (1978) classification, with modifications suggested in Sorriso-Valvo and Gullà (1996a) and Bisci et al. (1996). In order to avoid classes with too few cases, some types were grouped together and eventually the following seven types remained: 1) fall/topple; 2) block slide; 3) slide (either rock or earth); 4) complex (Varnes, 1978) slide/flow and flow; 5) lateral spreading; 6) sackung (rock flow); 7) debris avalanche.

The landslide zone class indicates areas where clustering of phenomena is so tight that it is impossible to distinguish different bodies, or several phenomena are too small to be mapped. They cover a considerable portion of the territory, especially on low-gradient slopes carved in clayey deposits, and mainly consist of slide-flow phenomena.

The detected 3359 mass movement phenomena affect a surface of 189 km^2, i.e. 22.1% of the study area (Fig. 2). Table 1 shows the incidence of each type of mass movement.

2.2.2. Lithology (LTU)

From the 1:25,000 scale geological map of Calabria (Burton, 1971), which is actually a litho-stratigraphic map, 13 lithologic units (LTU) were defined grouping rock types that present similar compositional and mechanical characteristics. In order to check for possible mistakes in the original map and solve problems concerning borderline rock types, it was necessary to carry out a field survey. The LTU determined (Fig. 3A) are:

- L— Loose deposits, made of alluvial and coastal sediments. Mainly continental; some are terraced.
- PLT— Terrace deposits Pleistocene in age. Reddish conglomerates and sands; marine at the base, now and then ending with continental layers (beach dune sands, debris-flow and alluvial fan sediments).
- C— Mainly clayey sediments. Clay, silty and sandy clays with layers of sands, silts or marls.
- S— Mainly sandy sediments. Sands with soft sandstones, with levels of silts or silty clays.
- CGL— Loose conglomerates with sandy matrix and occasional sandy layers.
- CGH— Hard conglomerates with calcarenites and quartzarenites. Jointed.
- EV— Evaporites, essentially gypsum and subordinate limestone. Intensively jointed and folded. Karst forms.
- AV— "*Argille Varicolori*", multi-coloured clayey melange. Chaotic structure.
- LJ— Limestones Jurassic in age, well layered. Jointed, karst forms.
- PLU— Plutonites, essentially granite and tonalite, in plutons and dykes. Jointed and deeply weathered.
- MMH— Medium to high-grade metamorphites. Essentially gneisses, biotite schists, amphibolites and migmatite gneisses. Jointed, folded and deeply weathered.
- HG— Haugen gneiss. Jointed and weathered.
- MLM— Low to medium-grade metamorphites. Essentially shales and phyllites. Jointed, folded, weathered.

Territorial frequency of LTUs is shown in Table 2.

Table 1
Mass movement incidence

Type	S. (km^2)	(%)
Landslide zone	75.03	39.67
Slide	34.17	18.07
Sackung	30.33	16.04
Slide/flow and flow	27.26	14.41
Debris avalanche	18.58	9.82
Block slide	3.02	1.59
Fall/topple	0.53	0.28
Lateral spreading	0.19	0.10
Total	189.12	100.00

2.2.3. Tectonic structures (STRU)

Faulting, folding and jointing are widespread throughout the study area. Major faults were mapped in order to introduce the distance from fault variable among the other relevant variables for recording the territorial distribution of mass movements (Sorriso-Valvo, 1989; Sorriso-Valvo and Tansi, 1996b). The geostructural analysis was performed through the interpretation of aerial photos ("*Italia*" flight 1:75,000 scale; and IGM flights 1:33,000 and 1:25,000 scale) and a field survey (Fig. 3B). Major normal and thrust faults were surveyed and mapped, except in the clayey melange zone where mapping is impossible due to their chaotic structure.

2.2.4. Land Use (LUS)

In a landslide-dominated area such as southern Calabria, land use is dependent on mass movements, thus this variable is normally found to be significantly associated with mass movements (among others, Carrara et al., 1978), even though this relationship is not simple.

Data on land use were obtained from digital maps of Corine-Land Cover project (APAT, 2005). The map is made from remotely detected data combined with

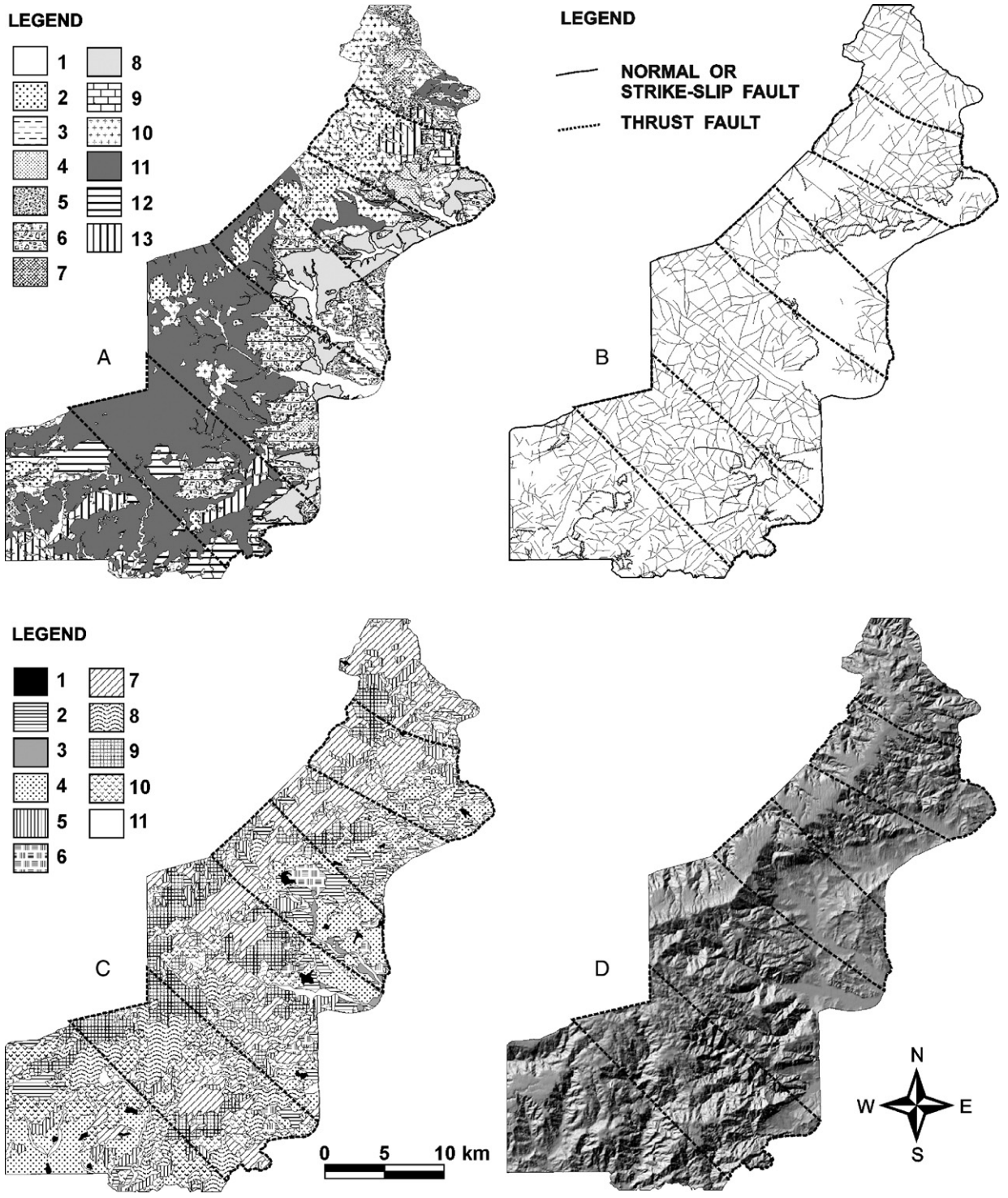

Fig. 3. Aspromonte study area geological, structural and morphological settings; in each map are located the sampling zones (40%). (A) Lithological map: 1 = Loose deposits (L); 2 = Terrace deposits Pleistocene in age (PLT); 3 = Mainly clayey sediments (C); 4 = Mainly sandy sediments (S); 5 = Loose conglomerates (CGL); 6 = Hard conglomerates (CGH); 7 = Evaporites (EV); 8 = Multi-coloured clayey melange of Argille Varicolori formation (AV); 9 = Limestones Jurassic in age (LJ); 10 = Plutonites (PLU); 11 = Medium to high-grade metamorphites (MMH); 12 = Haugen gneiss (HG); 13 = Low to medium-grade metamorphites (MLM). (B) Structural map. (C) Land use map: 1 = Urban area (UA); 2 = Arable land (AL); 3 = Orchards (O); 4 = Olive groves (OG); 5 = Pasture (P); 6 = Heterogeneous cultivation land (HCL); 7 = Deciduous forest (DF); 8 = Coniferous forest (CF); 9 = Mixed forest (MF); 10 = Mediterranean *macchia* (MM); 11 = Scarcely vegetated to bare (SVBL). (D) Shaded-relief.

Table 2
Distribution of lithological units (LTU) in the study area

LTU	S. (km^2)	(%)
MMH	319.10	37.70
PLU	92.44	10.90
AV	74.80	8.84
CGH	70.12	8.29
PLT	57.76	6.83
L	50.54	5.97
HG	45.40	5.37
MLM	42.76	5.05
S	37.65	4.45
C	30.65	3.62
CGL	17.94	2.12
LJ	5.82	0.69
EV	1.03	0.12

the results of a field survey. The nominal scale of the map is 1:100,000. CLC maps are actually organised into three levels of increasing detail. For this study, the layer of highest detail was used. The resulting layers in our GIS include 11 non-parametric values (Fig. 3C): 1) Urban area (UA); 2) Arable land (AL); 3) Orchards (O); 4) Olive groves (OG); 5) Pasture (P); 6) Heterogeneous cultivated land (HCL); 7) Deciduous forest (DF); 8) Coniferous forest (CF); 9) Mixed forest (MF); 10) Mediterranean *macchia* (MM); 11) Scarcely vegetated to barren land (SVBL).

Territorial frequencies of LUS are shown in Table 3.

2.2.5. Topographic features (ELEV, SLO, ASP, ACUR, DCUR)

In order to represent topography, a DEM and its derivate variables were adopted. Georeferencing is based on Gauss–Boaga coordinates; the square-grid has a 10 m side cell (Fig. 3D) obtained by mathematical processing of a 40-m cell DEM which also required careful amending due to a number of errors in elevation (e.g., the elevation of a bridge instead of that of the stream beneath). The interpolation function is bi-linear. For a portion of the study area, a 20 m side cell DEM of 600×600 points is available. It covers ca. 144 km^2. Performing the regression of 10 m interpolated DEM on this points DEM, we obtained the regression equation $I = T - 0.081$, where I = iterpolated and T = true, the correlation coefficient $r = 0.998$. The interpolation is thus reliable. The variable elevation (ELEV) is thus directly obtained.

Four more variables were obtained through the DEM: gradient (SLO), aspect (ASP), down-slope (DCUR) and across-slope curvature (ACUR). All these derived variables are associated with mass movements to a different degree. Slope angle, in particular, is consistently found to be highly relevant, but its relationship with the incidence of mass movements is not monotonic, as the maximum relative frequency of mass movements corresponds to intermediate slope angle values, even when slope angle concerns a unique rock type (Carrara et al., 1978, 1982; Iwahashi et al., 2003). Aspect essentially plays an important role in the frequency of shallow landslides favouring their presence on north-facing slopes, while low values of down-slope and across-slope curvature are associated with mass movements (Carrara et al., 1982).

Derived variables have been calculated for each 10 m cell, using spatial coordinates of 16 nodes of the cell and eight adjacent cells.

Each derived topographic map consists of 8,460,000 cells; values are floating point number. For the following analysis, the data have been grouped into classes.

Elevation classes are 100 m wide. The histogram in Fig. 4A shows their frequency distribution and displays two modes corresponding with the 700–800 m and 1100–1200 m elevation intervals.

Slope gradient, expressed as a percentage, was divided in ten isofrequential classes. Isofrequency avoids differences in relative weights and constitutes an objective criterion when defining class amplitude (Suzen and Doyuran, 2004). The classes so obtained are rather small in amplitude (except for the last class that is the most extended one) and do not differ substantially, so this help the analysis of the relationships between slope angle and mass movements.

Aspect has been subdivided into five classes: north, including azimuths between 315° and 45°; east, including azimuths between 45° and 135°; south, including azimuths between 135° and 225°; west, including azimuths between 225° and 315°; and horizontal. Frequency distribution is shown in Fig. 4B.

The curvature of cell surface was divided into three classes: flat, concave, convex. Values of the variables were obtained by mathematical intersection of the

Table 3
Distribution of land use categories (LUS) in the study area

LUS	S. (km^2)	(%)
DF	184.89	21.85
OG	130.06	15.37
CF	127.87	15.12
MF	124.86	14.75
MM	109.86	12.98
AL	58.47	6.92
P	51.76	6.11
SVBL	25.51	3.02
HCL	22.36	2.64
O	5.21	0.62
UA	5.23	0.62

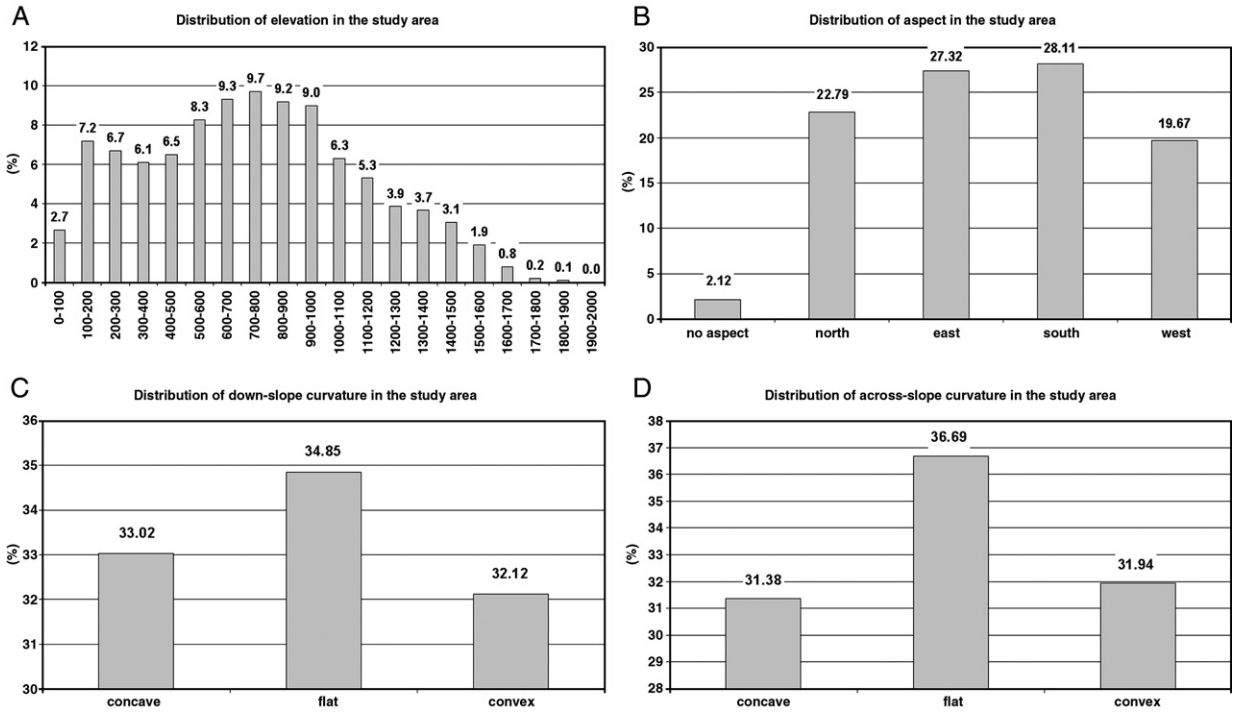

Fig. 4. Distribution of topographic features in the study area: A) elevation (ELEV); B) aspect (ASP); C) down-slope curvature (DCUR); D) across-slope curvature (ACUR).

ground surface with a vertical plane set along the direction of maximum slope (DCUR), and orthogonally to it (ACUR). Flat cells prevail in both DCUR (Fig. 4C) and ACUR (Fig. 4D).

All the data are organized in layers on a GIS. The cells have the same size as DEM (10 m). The GIS are implemented on a UNIXS O.S. by means of ARC-Info 6.2 package (ESRI, 1991).

3. Evaluation of landslide susceptibility

In this section, the sampling procedure is described first, then there is a description of two applications, first without distinguishing the typology of mass movements, and then for selected types of mass movement.

3.1. Procedure

Once the data-base is implemented, the procedure for evaluating landslide susceptibility can be initiated by following the four steps of sampling, variables parameterisation, model fitting and application.

The LR procedure in-built in the ARC-Info 6.2 package can be used for the analysis. This makes it possible to handle data sets easily and incorporate them in the analysis.

3.1.1. Sampling

LR sampling consists in obtaining values of independent variables from a sample zone which is

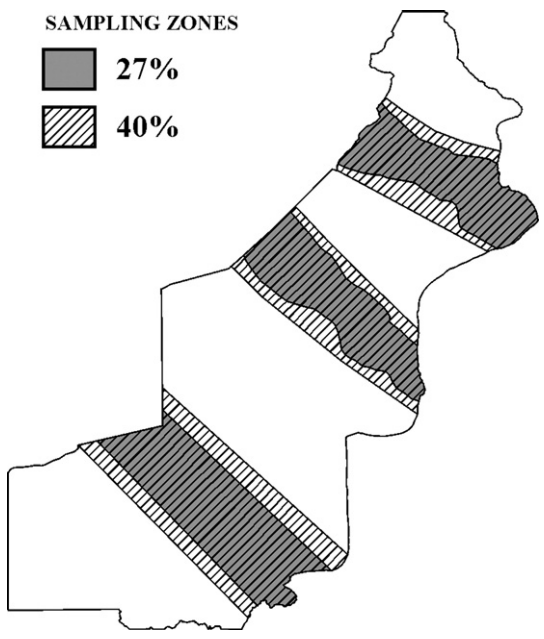

Fig. 5. Location of sampling zones in the study area.

Table 4
Reclassification index of independent variables LTU, LUS, ELEV, SLO, ASP, ACUR and DCUR referred to: A = undifferentiated landslides; B = slide; C = debris avalanche

	A	B	C
LTU			
L	0	0	0
PLT	7	0	5
C	516	16	4
S	334	13	57
CGL	375	12	23
CGH	175	11	62
EV	717	83	44
AV	959	2	5
LJ	502	52	0
PLU	129	8	176
MMH	155	12	127
HG	96	9	83
MLM	220	23	168
ELEV			
0–100	178	19	0
100–200	648	14	8
200–300	754	32	21
300–400	613	49	25
400–500	287	65	70
500–600	171	54	108
600–700	167	49	132
700–800	154	58	184
800–900	124	55	176
900–1000	84	37	90
1000–1100	97	29	91
1100–1200	123	37	162
1200–1300	111	27	150
1300–1400	40	17	61
1400–1500	8	5	8
1500–1600	3	2	8
1600–1700	0	0	0
1700–1800	0	0	0
1800–1900	0	0	0
1900–2000	0	0	0
ACUR			
Concave	286	44	149
Flat	260	36	62
Convex	246	35	53
LUS			
UA	499	4	0
AL	724	18	8
O	225	3	131
OG	520	41	46
P	190	36	48
HCL	609	20	3
DF	124	53	124
CF	96	23	102
MF	56	16	91
MM	226	68	138
SVBL	195	69	162
SLO			
<10%	170	5	3
10%–16%	417	13	8
17%–23%	471	21	15
24%–31%	366	31	36
32%–40%	241	43	69
41%–47%	197	57	109
48%–55%	186	61	144
56%–64%	180	60	179
65%–75%	178	61	203
>75%	164	52	182
ASP			
Horizontal	50	2	1
North	219	47	77
East	268	39	75
South	299	39	107
West	275	31	91
DCUR			
Concave	239	36	72
Flat	286	39	71
Convex	265	41	118

representative of the remaining area to which LR will be applied.

Sampling is a critical step, as the reliability of the whole procedure depends on its accuracy. Nevertheless, this step is not performed univocally (Ayalew and Yamagishi, 2004).

In this paper, we introduce a procedure aimed at obtaining a classification of the territory (probability of occurrence of mass movements) on the basis of a reliable sample area obtained by the careful mapping of a portion of the study area.

Sampling zones must be representative of the entire study area, but at the same time they should be small enough to minimise cost and time.

In order to define the extent and shape of the sampling zone, several tests were made in a test basin (included in the study area), the Laverde torrent, extending approximately over 70.5 km^2. Tests revealed that LR coefficients, obtained in the sampling zone of the test basin, remain close to those obtained in the whole basin, if the sampling zone is at least 25% of the whole test basin. In addition, the sampling zone should be shaped like stripes running parallel to the general slope direction of the study area (Guarascio et al., 2005).

As Aspromonte is a rugged and varied land, two different sets were individuated each one including three transects parallel to the dip of the general slope of the study area (Fig. 5). One set covers an area of ca. 231 km^2 (ca. 27% of the whole study area), the other one

extends over 340 km^2 (ca. 40% of the whole study area); the 40% zone includes the 27% one. The purpose of this double sampling is to compare the results from zones of different sizes.

In order to achieve the aims of this paper, the mapping of mass movements in these transects had to be as accurate as possible. In the 27% sample zone 1108 mass movement phenomena were detected, extending over 26.4% of this sample area. In the 40% sample zone, phenomena are 1617 and extend over 29.6% of the sample zone.

In the GIS-related data-base, data constitute the set in which each cell is a record. Every record is a vector in which a progressive id-index, cell coordinates, the value of dependent and independent variables are stored.

3.1.2. Reclassification and parameterisation

Logistic regression is applied to dichotomic dependent variables, thus the classification variable "mass-movement type" (or "mass movements" when dealing with undifferentiated phenomena) must be reclassified as 1, for cells where the phenomenon exists, and 0 for cells where it does not.

Independent variables should be parametric and their relationships with dependent variables should be linear. Non-parametric variables can be quasi-parametric if their values are ranked on an absolute scale based on the mass movements incidence on each variable class (Carrara et al., 1982). This can be done on the basis of the data from the sampling zones.

Similarly, parametric independent variables may display non-linear relationships with dependent variables (e.g. landslide frequency vs. slope angle, Carrara et al., 1978, 1982; Iwahashi et al., 2003). In such cases, classes of independent variables are re-arranged by means of mass movements relative frequency, in order to make the relationships with the dependent variable linear, or at least monotonic.

Mass movements relative frequency values used for the parameterisation and reclassification (reclassification index) of independent variables are shown in Table 4, where frequency values have been multiplied by 10 in order to shorten computing time; thus, all variables range from 0 to 100.

LR analysis is rather robust as concerns normality of frequency distribution of values of independent variables, thus no variable transformation is required.

3.1.3. Fitting

LR fitting consists in defining statistical linear relationships between presence/absence of mass movements and independent variables. In this step, the computing program assigns all possible weights to the regression independent variables by means of an iterative procedure, until the root mean square residuals in the regression are minimised. At the end of this step, the program provides regression weights (a_i), RMSE (Root Mean Square Error) and Chi-square. To evaluate the goodness of the fit, RMSE must be minimised and Chi-square maximised.

3.1.4. Application

If RMSE and Chi-squared values are satisfactory, the assessment logistic function can be extended to the entire study area, where only independent variables values are known.

By means of this step, the value of $P(y)$ is assigned to each cell, i.e. the probability that any given cell is affected by mass movements. As this probability is determined on the basis of land characteristics, territorial susceptibility to mass movements is actually determined.

The output of this application is a grid of floating point values between 0 and 1. The precision is to the third decimal number. In order to render the resulting file easier to handle, the data are grouped in 10 equal-amplitude probability classes, expressed as a percentage (0% to 100%).

At this step the entire territory is classified in terms of probability of occurrence of any kind, or of a specific kind of mass movement.

3.2. Landslide susceptibility evaluation for undifferentiated landslides

In this case, no distinction is made between types of landslide. Landslide zones are included in the sampling step.

Reclassification and parameterisation of variables are shown in Table 4. Regression weights determined in the fitting step are: $a_0=-6.073$; $a_1=0.004$; $a_2=0.000$; $a_3=0.003$; $a_4=-0.001$; $a_5=0.003$; $a_6=0.009$; $a_7=0.001$; where a_0 is the intercept and a_i are the weights of the variables LTU (a_1), LUS (a_2), ELEV (a_3), SLO (a_4,), ASP (a_5), ACUR (a_6) and DCUR (a_7) respectively. There are just three decimal numbers displayed, but the computing program works with a much higher precision.

The coefficient of the variables STRU is nearly 0; in addition, RMSE and Chi-square worked better when this variable was excluded. Thus, in contrast with findings in other case studies (Anbalagan and

Singh, 1996; Sorriso-Valvo and Tansi, 1996b; Ercanoglu and Gokceoglu, 2004), but in agreement with previous studies performed in this area (Carrara et al., 1982), geological structures do not affect landslide variability, as a result they do not appear in the list above.

In this analysis, RMSE = 0.347 and Chi-square = 278,473. These values indicate a good accuracy in the

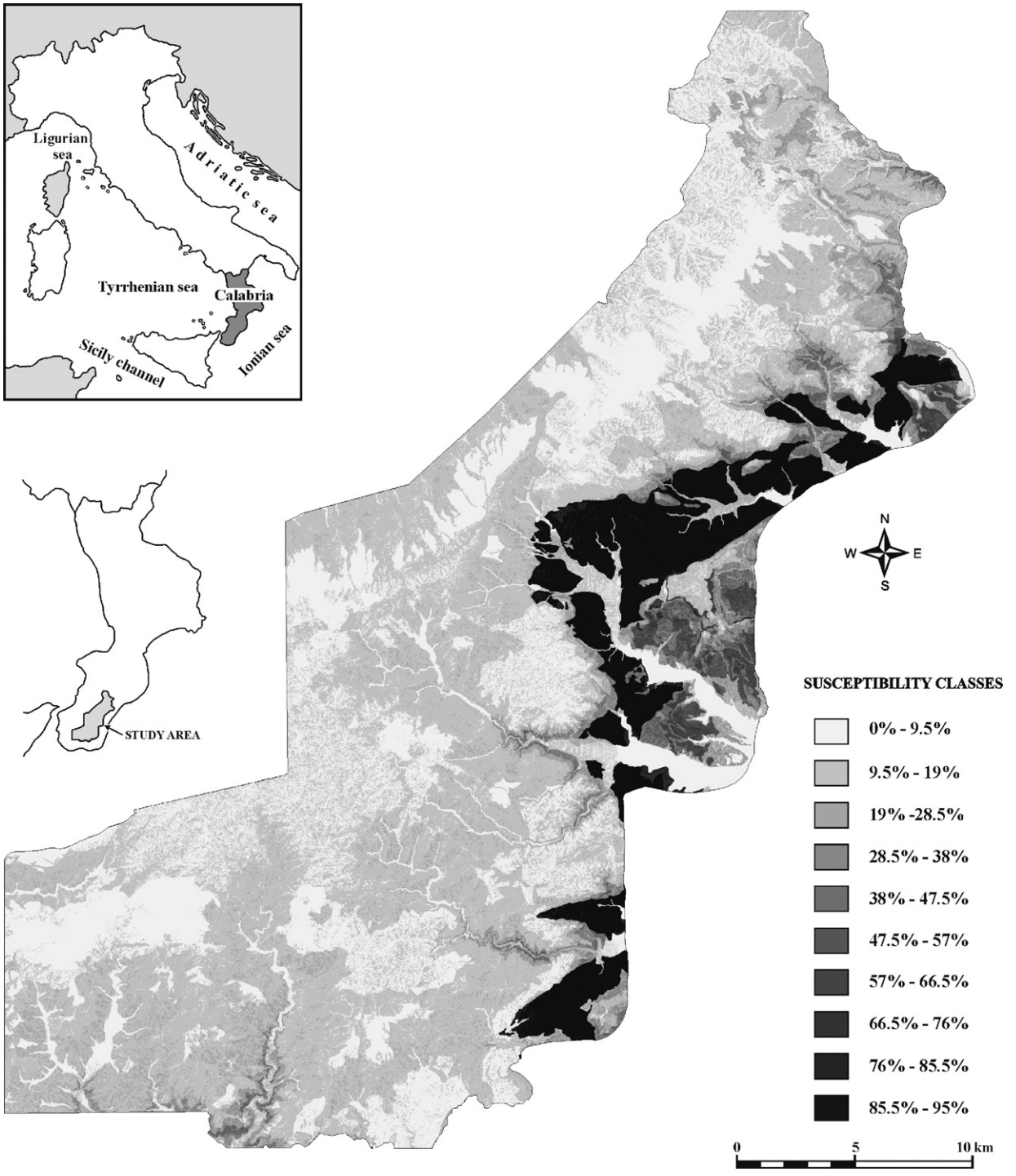

Fig. 6. Susceptibility map for undifferentiated landslides.

estimate and a significant connection between the dependent variable and the independent ones.

For this LR analysis, $P(y)$ values range from 0 to 95%; the susceptibility map obtained with the 27% sampling area is shown in Fig. 6.

3.3. Landslide susceptibility evaluation for different types of mass movement

The territorial distribution of mass movements also depends on the typology of phenomena, which in turn is

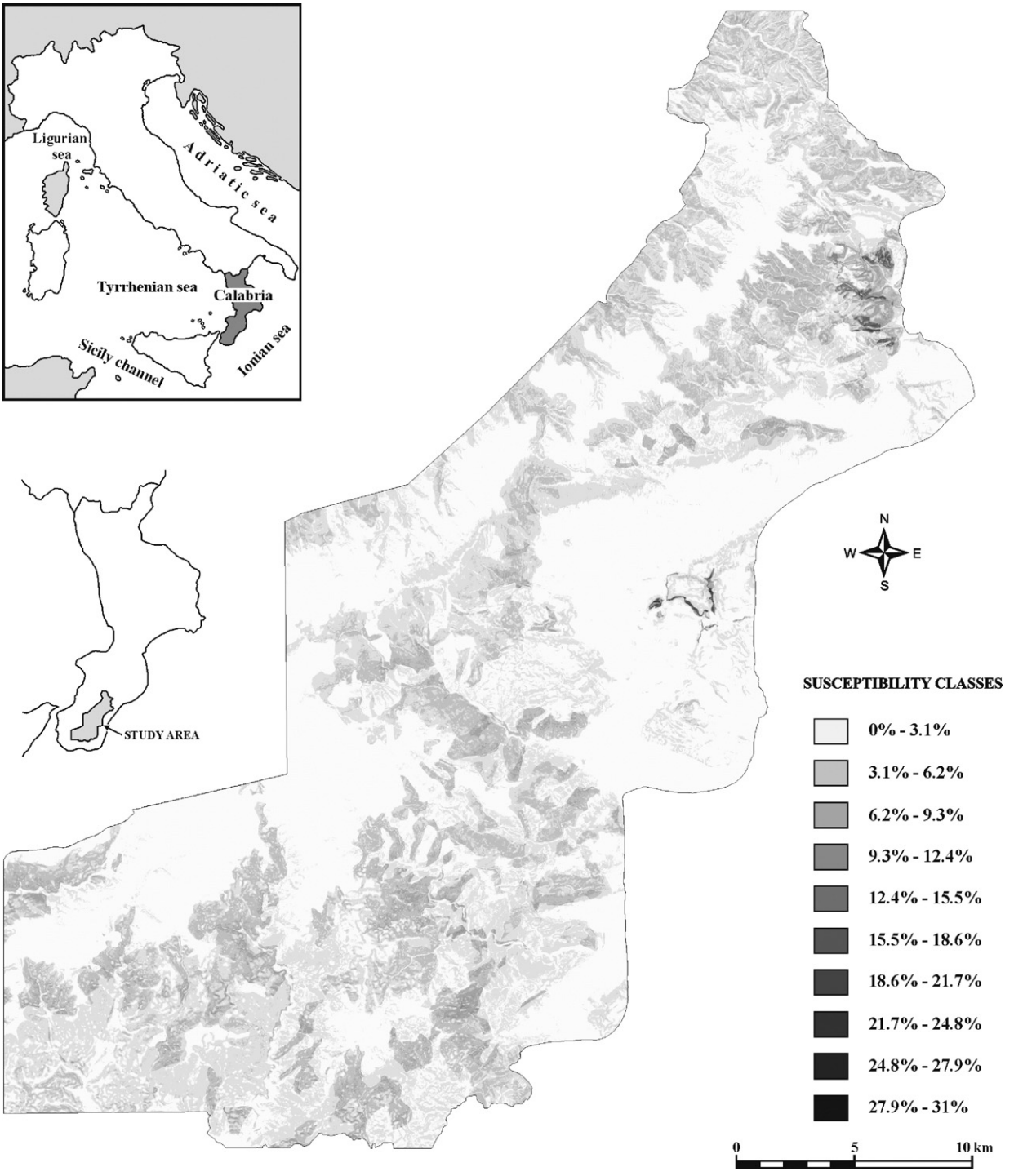

Fig. 7. Susceptibility map for slide.

closely linked with slope lithology (e.g. earth flows are typical of clayey rocks) and morphology (falls occur on very steep slopes).

Susceptibility was evaluated for every type of mass movement, excluding those represented by a very limited number of cases (lateral spreading, topple, fall).

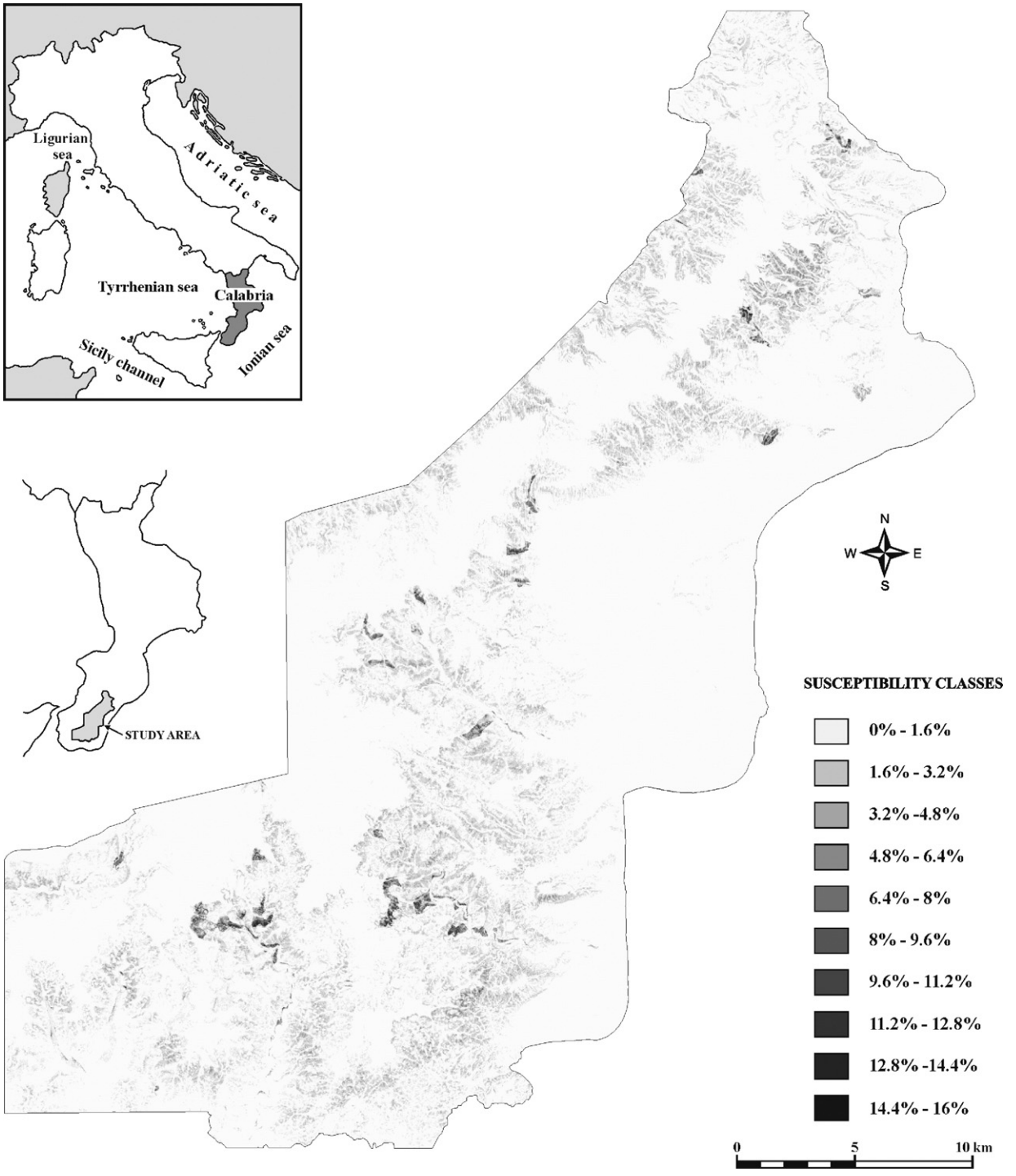

Fig. 8. Susceptibility map for debris avalanche.

Table 5
Regression weights and value of RMSE and Chi-square obtained through logistic regression performed on: A = slide; B = debris avalanche

Reg. weights.	*A*	B
a_0	−7.626	−8.298
a_1	0.002	0.003
a_2	0.002	0.000
a_3	0.001	0.006
a_4	0.002	0.008
a_5	0.002	0.007
a_6	0.001	0.011
a_7	0.002	0.000
RMSE	0.191	0.092
CHI^2	84,241	19,589

a_0 (intercept); a_1 (LTU); a_2 (LUS); a_3 (ELEV); a_4 (SLO); a_5 (ASP); a_6 (ACUR); a_7 (DCUR).

The performance of this procedure was estimated in the validation step. The results are statistically significant for slide and debris avalanche types. Reclassification and parameterisation of variables are shown in Table 4. Regression weights, RMSE and Chi-square values are shown in Table 5. For slides, $P(y)$ values range from 0 to 0.31, and the slide-susceptibility map is shown in Fig. 7. For debris avalanche, $P(y)$ values range between 0 and 0.16. Fig. 8 shows the susceptibility map for this type of phenomena. Sackung and slide-flows susceptibility maps are not displayed, as the results of LR were not significant for sackung and slide-flow phenomena.

4. Validation

In order to validate the prediction capability of the adopted sampling procedures and to test the representativeness of the selected sampling zone (27%), the LR procedure was extended to the whole study area and to the larger sampling zone covering 40% of the whole study area.

The results of the LR analysis when extended to the whole study area represent the best possible capability of LR in predicting the probability of the existence of mass movements phenomena. The results of the sampling LR analysis when performed on the extended sampling zone (40%) are expected to represent an intermediate position, between that of the 27% sampling procedure and that of the whole area.

Then, the results of each sampling procedure were compared with ground truth, and those based on sampling zones (27% and 40%, respectively) with those of the 100% sampling area.

The comparison between results of LR procedures and ground truth was carried out by performing a simple linear regression of expected values of probability for the different types of mass movement, with respect of observed values, i.e. the percentage of cells actually affected by mass movements for each probability class. The percentage of cells correctly classified was also determined, by comparing cell by cell the value of expected and actual value of $P(y)$. In this case the spatial correspondence is determined.

4.1. Comparing the whole area sampling procedure with ground truth

The results of this regression are shown in Fig. 9 and Table 6a.

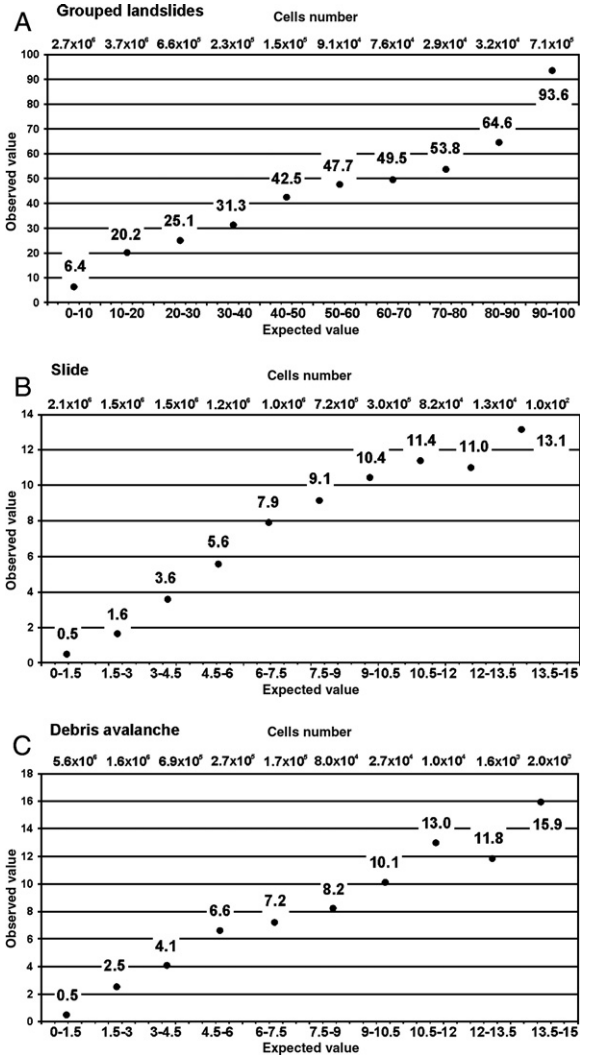

Fig. 9. Comparison between expected values of extended procedure and ground truth: A) undifferentiated landslides; B) slide; C) debris avalanche.

Table 6
a) Regression of expected values of probability with respect to that observed, for extended procedure; b) regression between observed values of probability obtained with 27% sampling procedures, with 100% sampling procedure; c) regression between observed values of probability obtained with 40% sampling procedures, with 100% sampling procedure; d) regression of expected values of probability with respect to observed values, for the 27% sampling procedure; e) regression of expected values of probability with respect to observed values, for the 40% sampling procedure

	R	s
a) 100% vs. ground truth		
Undifferentiated landslides	0.96	1.18
Slide	0.98	1.02
Debris avalanche	0.99	0.92
b) 27% vs. 100%		
Undifferentiated landslides	0.97	1.06
Slide	0.45	0.90
Debris avalanche	0.84	0.63
c) 40% vs. 100%		
Undifferentiated landslides	0.97	1.06
Slide	0.81	0.85
Debris avalanche	0.91	0.83
d) 27% vs. ground truth		
Undifferentiated landslides	0.97	1.04
Slide	0.45	0.48
Debris avalanche	0.90	1.20
e) 40% vs. ground truth		
Undifferentiated landslides	0.95	1.01
Slide	0.76	0.86
Debris avalanche	0.94	1.04

R=correlation coefficient; s=regression line slope.

Regression of expected vs. observed values of landslide frequency for every type of phenomena (Fig. 9A) produced a correlation coefficient $R=0.96$, and a regression line slope $s=1.18$ (Table 6a), indicating a good performance.

A comparison of cases correctly classified with cases misclassified is shown in the confusion matrix of Table 7, where 83.5% of cases are correctly classified if the value of $P(y)=0.50$ is taken as threshold for landslide ($P(y)\geq 0.50$) and non-landslide ($P(y)<0.50$) cells.

When considering the different types of phenomena, the results are as follows:

In general slides, the scattergram (Fig. 9B) is positively monotonic, except for the 12–13.5% class. $R=0.98$ and $s=1.02$.

The debris avalanche scattergram (Fig. 9C) is not regularly monotonic. $R=0.99$, $s=0.92$.

$P(y)$ is, however, much lower than 0.50 (Fig. 9B and C) for slide and debris avalanche cases, no single cell can be classified as a landslide cell, while there is a considerable number of cells that are actually affected by slide or debris avalanche; so one cannot make a confusion matrix as in the case of undifferentiated phenomena. Thus the LR failed to detect mass movements cells when typology was considered. Nevertheless, recalling the above simple regression analyses, it is clear that the actual observed frequency is nearly equal to the estimated probability $P(y)$ in each probability class (Fig. 9B and C). Thus LR appears as a good estimator of mass movements frequency (which is, of course, true also for undifferentiated phenomena), even though it cannot predict which cell will be affected by slide or debris avalanche.

Table 7
Confusion matrix

	Observed true		Observed false			Total	
	n	%	*n*	%		*n*	%
a) Sample 100%							
$P(y)<50\%$	1,228,319	16.4	**6,273,392**	**83.6**	Correct	7,065,114	83.5
$P(y)>50\%$	**791,722**	**82.8**	164,652	17.2	Incorrect	1,392,971	16.5
b) Sample 27%							
$P(y)<50\%$	1,206,491	16.2	**6,261,947**	**83.8**	Correct	7,075,497	83.7
$P(y)>50\%$	**813,550**	**82.2**	176,097	17.8	Incorrect	1,382,588	16.3
c) Sample 40%							
$P(y)<50\%$	1,180,805	16.0	**6,196,595**	**84.0**	Correct	7,035,831	83.2
$P(y)>50\%$	**839,236**	**77.7**	241,449	22.3	Incorrect	1,422,254	16.8

Total correct and incorrect cells for undifferentiated landslides. True cells are those with mass movement. False otherwise. Value (true of false) of each real cell is compared with probability estimated by LR ($P(y)$). Read the matrix along the rows; correct cells number and percentage in boldface.

4.2. Comparing the 27% and 40% sampling procedures with the 100% sampling procedure

The results of standard (27%) and enlarged (40%) sampling procedures are now compared with the best possible results obtained with the 100% procedure performed using the reclassification index obtained from the whole study area.

The obtained correlation coefficient (R) and regression line slope (s) are listed in Tables 6b and c.

This comparison indicates that the results of standard sampling were actually close to that of the extended LR as regards to all types of mass movements ($R=0.97$) and debris avalanche ($R=0.84$), while it appears not very good for slide ($R=0.45$). As regards the 40% sampling, all the results are close to that of the 100% sampling for grouped mass movement types ($R=0.97$), slide ($R=0.81$), and debris avalanche ($R=0.91$).

4.3. Comparing the 27% sampling procedure with ground truth

The results of this comparison are shown in Fig. 10A, B and C, and Table 6d.

For grouped mass movements, the frequency distribution monotonically increases as shown in Fig. 10A.

The regression of expected vs. observed values of probability produced a correlation coefficient $R=0.97$, and the regression line slope $s=1.04$ (Table 6d), indicating a very good performance. The confusion matrix for 27% sampling area gives an even better result numerically but it is essentially equivalent to that of 100% sampling area (Table 7b).

As regards the different types of phenomena:

The slides scattergram (Fig. 10B) increases monotonically except for the highest class (27.9–31%) that displays a net fall, the correlation coefficient $R=0.45$ and the regression line slope $s=0.48$ (Table 6d). This regression yielded poor results.

The debris avalanche scattergram (Fig. 10C) increases monotonically, with $R=0.90$ and $s=1.20$ (Table 6d). This result is fairly good, even though limited to the estimation of spatial frequency, not to cells identification.

The sackung scattergram (not shown) is irregular. $R=-0.57$ and $s=-1.21$, neither achieves a good agreement between the estimated and real spatial probability (frequency) of events.

The slide-flows scattergram (not shown) increases monotonically, $R=0.90$ and $s=1.25$. The value of s is rather high, but the result should be considered as fairly good in terms of spatial frequency estimation.

4.4. Comparing the 40% sampling procedure with ground truth

Fig. 11A, B and C, and Table 6e show the results of these regressions.

For all types of phenomena, the performed regression of expected vs. observed values of landslide frequency (Fig. 11A) produced a correlation coefficient $R=0.95$, and a regression line slope $s=1.01$ (Table 6e), indicating a good predictive performance. This is confirmed by the confusion matrix (Table 7c) that indicates 83.2% of cases correctly classified.

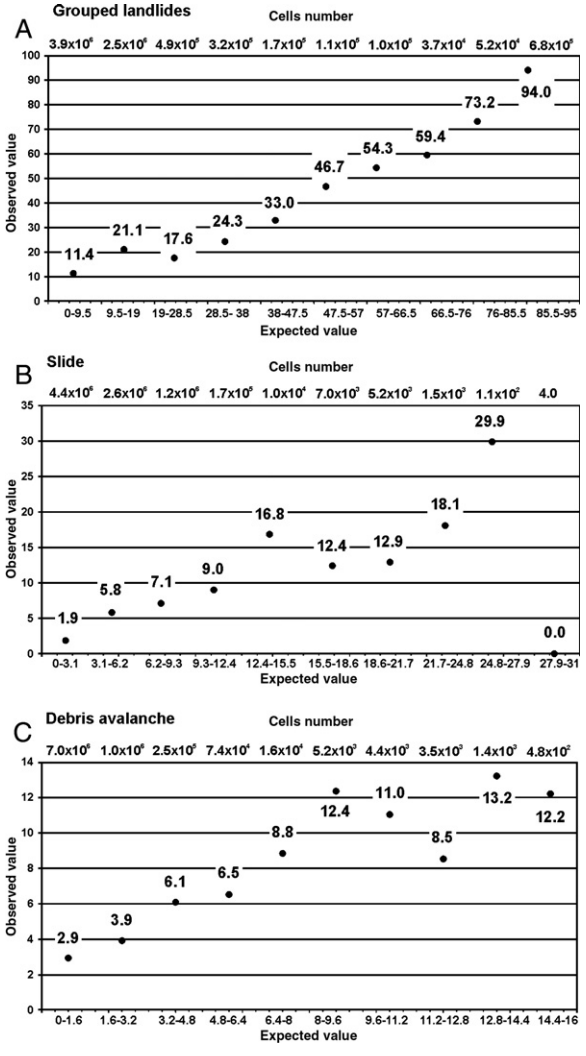

Fig. 10. Comparison between expected values of the 27% sampling procedure and ground truth: A) undifferentiated landslides; B) slide; C) debris avalanche.

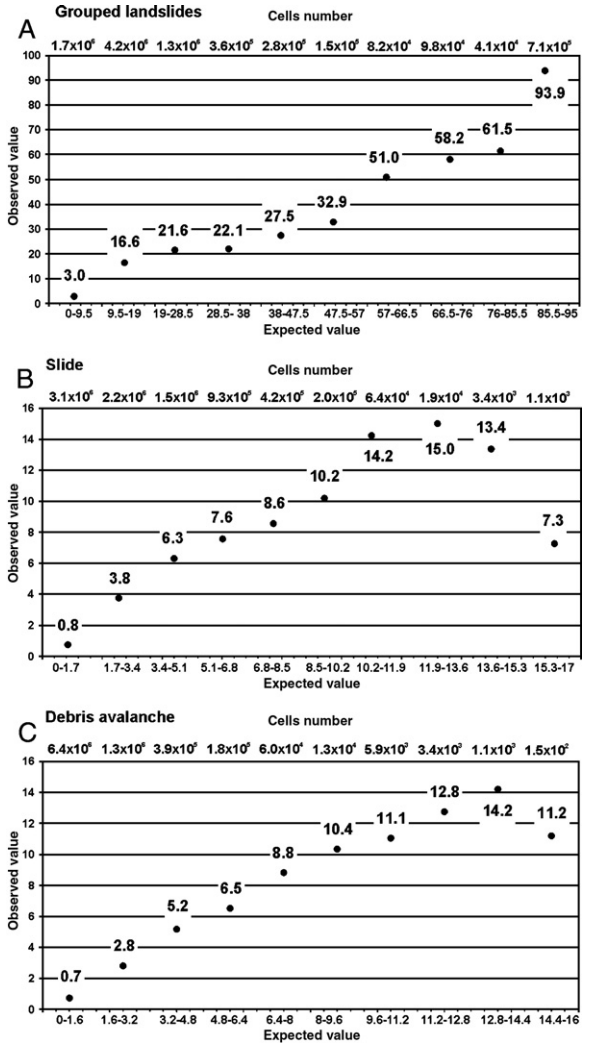

Fig. 11. Comparison between expected values of the 40% sampling procedure and ground truth: A) undifferentiated landslides; B) slide; C) debris avalanche.

As regards to the different types of phenomena, results are as follows:

The slides scattergram (Fig. 11B) increases monotonically up to the 11.9–13.6% class, and then decreases, with $R=0.76$ and $s=0.86$. This performance is fair as regards to the relative frequency estimation, but not landslide identification.

The debris avalanche scattergram (Fig. 11C) is in general monotonic, with a decrease located in the last class (14.4–16%). $R=0.94$, $s=1.04$. This performance is good, in terms of relative frequency estimation, but not for landslide cells identification.

The sackung scattergram (not shown) increases monotonically, but is rather irregular, so that $R=0.59$ and $s=0.06$. These results are not good, even if they are better than those of the 27% sampling procedure.

The slide-flow scattergram (not shown) is irregular; $R=0.49$ and $s=0.16$, a very bad result, much worse than that obtained with a 27% sampling area. This unexpected result implies that the statistics is not linearly affected by the sampling size. Of course, the fair results of the 27% sampling should not be considered reliable.

5. Discussion and conclusions

In selecting the study area to apply LR to evaluate the probability of existence of mass movements based on ground characteristics, the authors decided to keep the variables to a minimum possible number but, within the limitations imposed by time and finance, selected an extensive area as possible in order to maximise sample populations. In fact, the whole study area extends over 850 km^2 and the sampling areas over 231 (27%) and 340 km^2 (40%), respectively.

The study was conducted by means of a square-grid based GIS. The size of the grid cell is 10 m on the ground, and is derived by mathematical processing of a 40 m cell grid.

The variables selected for the analysis were: lithology, distance from major fault, slope altitude, gradient, aspect and curvature (both down slope and across-slope), and land use. Distance from a major fault, which was relevant in different case studies (Anbalagan and Singh, 1996; Sorriso-Valvo and Tansi, 1996b; Ercanoglu and Gokceoglu, 2004) turned out to be absolutely irrelevant and was, thus, excluded from the analysis.

Non-parametric variables (lithology, land use) were transformed into grouped parametric ones and the mass movements frequency observed in the sampling zone assigned to the non-parametric class of each variable.

Slope gradient displays a non-linear relationship with relative frequency of mass movements, thus its classes were ordered according to the observed relative frequency of mass movements. This also minimised the problem of a too sudden increase of amplitude in the final classes which actually corresponds to a moderate increase in slope angle.

In this procedure LR works in a similar way to an artificial neural network when the computing program performs a sort of “learning” by iteration.

From the analysis of the standardized coefficients of variables, it appears that cross-slope curvature, lithology, elevation and aspect are the most important ones for determining susceptibility to mass movement. Indeed,

the cross-profile of cells tends to be controlled by the presence of a landslide (Carrara et al., 1982). There is certainly nothing new in the recognition of the role of lithology in determining the presence of mass movements. In this study area, its highest and lowest parts are less affected by mass movement (Fig. 2); in general, north-facing slopes are more likely to be affected by mass movements, while south-facing slopes are more prone to erosion.

However, the aim of this work was to assess whether LR is able to distinguish landslide-affected zones from non-affected ones, using a limited number of independent variables, and this aim has been essentially achieved (Figs. 6 7 and 8).

The selection of sample zones in partial sampling procedure is critical, as demonstrated by the need for a set of trials with differently sized and shaped zones in order to find the most appropriate one, which, in this study, were strips parallel to the overall gradient of the study area.

As regards the practical application of the proposed procedure, it is clear that it requires that the mass movement phenomena in the sampling zone are carefully and thoroughly surveyed. In the case of the 100% sampling area procedure, the results were good for both undifferentiated (Fig. 9A and Table 6a) and slides and small-scale debris avalanches (Table 6a and Fig. 9B and C, respectively) in terms of the evaluation of mass movements spatial frequency; in terms of the classification of each single cell, however, the results were good only for undifferentiated phenomena (Table 7).

As regards the partial sampling procedure, the 27% zone produced satisfactory results for undifferentiated phenomena (Fig. 10A and Table 6d); as regards the single-cell spatial classification, the evaluation of relative frequency was acceptable for debris avalanches (Fig. 10C and Table 6d) but poor for slides. The results were similar when the sampling zone rose to 40% but, when dealing with the different types of mass movement, the evaluation of spatial frequency was acceptable for debris avalanches only (Fig. 11C).

The decline in performance of the LR procedure when dealing with differentiated types of mass movement, could also depend on the grid-based GIS. Indeed, the worse results for the individual typologies, are for sackung and slide-flows. Both phenomena show peculiar ground forms, but these forms are typically present in specific parts of the phenomena: trenches are typical for sackung upper parts, while convex slopes dominate in the lower parts of the phenomenon; but neither trenches nor convex slopes alone are indicators of the presence of a sackung-type deformation. In a slide-flow, the slide in the upper part of the phenomenon, has quite different forms compared with the flow in the lower part. As the adopted GIS is based on a small-cells grid (10 to 30 m in side), such different characters in the different parts of a mass movement body cannot influence the morphology of each single cell. As a consequence, LR cannot take advantage of all the morphological variables for probability assessment. This problem is less important for undifferentiated phenomena, because in this case a peculiar local morphology, together with other conditions (lithology, aspect, gradient, land use) are evidently relevant.

A polygon-based GIS should make it possible to overcome this problem, as many more elements can be used to characterize each polygon, so every polygon can have a wide variety of modes in which the various elements combine. In addition, their form and extent conform with physiographic units, including mass movement phenomena. Thus the fitting step of LR can be more effective than with square-grid cells.

The reliability of the analysis above is confirmed by the fact that the model is convergent as the sample zone increases, except for slide-flows. Indeed, if we limit the discussion only to the best cases, the confusion matrix and correlation of the results of the 27% sampling procedure, vs. those of the 100%, indicate that R and s range from 0.45 to 0.97 and from 0.63 to 1.06, respectively (Table 6b and c), with good results for undifferentiated phenomena, roughly acceptable results for debris avalanche, but poor for slides (for which $s=0.90$, but $R=0.45$); the results compared with a 40% sampling area, demonstrate that R and s range from 0.81 to 0.97 and from 0.83 to 1.06, respectively (Table 6b and c), displaying less divergence from the best possible results.

A further datum on procedure reliability is the comparison of results of 40% sampling zone with ground truth, when excluding sampling zones. In this case, R declines from 95% to 81%, while s varies just from 1.01 to 0.97. The decline is sensible but not substantial. We do not discuss this comparison in Section 4, because in LR validation sample area are normally included (Dai and Lee, 2002; Ohlmacher and Davis, 2003; Ayalew and Yamagishi, 2004).

Overall, it appears that the LR sampling procedure adopted in this paper describes well the probability of the presence of mass movement, and a sampling zone of about 27% of the study area, is sufficiently representative of the whole area, if the procedure is applied to undifferentiated types of mass movement. Some difficulties arise with single types of mass movement.

As regards to debris avalanche phenomena, a sampling zone of 27% of the study area remains sufficiently representative, while for slide phenomena a sampling zone of about 40% of the study area is necessary.

As the adopted variables are all ground variables, the assessment of probability can be considered as ground susceptibility to mass movements.

Acknowledgments

We thank two anonymous reviewers for their useful comments and suggestions. Language has been revised by K. O'Connell and we thank him too for improving our language.

References

Anbalagan, R., Singh, B., 1996. Landslide hazard and risk assessment mapping of mountainous terrains— a case study from Kumaun Himalaya, India. Engineering Geology 43, 237–246.

APAT, 2005. Project: Corine Land Cover 2000 Italy. Agenzia per la Protezione dell'Ambiente e per i servizi Tecnici, report n. 36/2005, 86 pp.

Ayalew, L., Yamagishi, H., 2004. The application GIS-based logistic regression for Landslide susceptibility mapping in the Kakuda–Yahiko Muuntains, central Japan. Geomorphology 65, 15–31.

Atkinson, P.M., Massari, R., 1998. Generalised linear modelling of susceptibility to landsliding in the Central Apennines, Italy. Computers & Geosciences 24 (4), 371–383.

Baeza, C., Corominas, J., 2001. Assessment of shallow landslide susceptibility by means of multivariate statistical techniques. Earth Surface Processes and Landforms 26, 1251–1263.

Berrnknopf, R.L., Brookshire, D.S., Shapiro, C.D., 1988. A probabilistic approach to landslide hazard mapping in Cincinnati, Ohio, with applications for economic evaluation. Bulletin of the Association of Engineering Geologists 24 (1), 39–56.

Bisci, C., Dramis, F., Sorriso-Valvo, M., 1996. Rock flow (Sackung). In: Dikau, R., Brunsden, D., Schrott, L., Ibsen, M.L. (Eds.), Landslide Recognition: Identification, Movement and Causes. IAG Publication, vol. 5, pp. 150–160.

Bonardi, G., Guerrieri, S., Messina, A., Perrone, V., Russo, M., Zappetta, A., 1979. Osservazioni geologiche e petrografiche sull'Aspromonte. Bollettino della Società Geologica Italiana 98, 55–73.

Brabb, E.E., 1982. Preparation and use of landslide susceptibility map for a country near San Francisco, California. In: Sheko, A. (Ed.), Landslide and Mudflows: Center of International Projects, Moscow, pp. 407–419.

Brabb, E.E., 1984. Innovative approaches to landslide hazard mapping. Proc. 4th International Symposium on Landslides, Toronto, vol. 1, pp. 307–324.

Brabb, E.E., Pampeyan, E.H., Bonilla, M.G., 1978. Landslide susceptibility in San Mateo Country, California. US Geological Survey Misc. Field Studies Map, MF-360, map at 1:62.500 scale.

Burton, A.N., 1971. Carta Geologica della Calabria (1:25,000)— Relazione Generale. Cassa per Opere Straordinarie di Pubblico Interesse nell'Italia Meridionale (Cassa per il Mezzogiorno), p. 120.

Carrara, A., 1983. Multivariate models for landslide hazard evaluation. Mathematical Geology 15 (3), 403–426.

Carrara, A., 1989. Landslide hazard mapping by statistical methods: a 《black-box》 model approach. In: Siccardi, F., Brass, R. (Eds.), International Workshop on Natural Disasters in European–Mediterranean Countries, Perugia, pp. 427–445.

Carrara, A., Guzzetti, F. (Eds.), 1995. Geographical Information Systems in Assessing Natural Hazard. Kluwer Academic Pub, Dordrecht, Holland, p. 342.

Carrara, A., Pugliese Caratelli, E., Merenda, L., 1977. Computer-based data bank and statistical analysis of slope instability phenomena. Zeitschrift für Geomorphologie N.F. 21 (2), 187–222.

Carrara, A., Catalano, E., Sorriso-Valvo, M., Reali, C., Osso, C., 1978. Digital terrain analysis for land evaluation. Geologia Applicata e Idrogeologia 13, 69–127.

Carrara, A., Sorriso-Valvo, M., Reali, C., 1982. Analysis of landslide form and incidence by statistical techniques, Southern Italy. Catena 9, 35–62.

Carrara, A., Cardinali, M., Detti, R., Guzzetti, F., Pasqui, V., Reichenbach, P., 1990. Geographical Information Systems and Multivariate Models in Landslide Hazard Evaluation. VI ICFL – ALPS 90, Milano 17–28.

Carrara, A., Cardinali, M., Detti, R., Guzzetti, F., Pasqui, V., Reichenbach, P., 1991. GIS Techniques and statistical models in evaluating landslide hazard. Earth Surface Processes and Landforms 16 (5), 427–445.

Carrara, A., Cardinali, M., Detti, R., Guzzetti, F., Pasqui, V., Reichenbach, P., 1992. Sistemi Informativi Geografici nella valutazione del rischio connesso all'instabilità dei versanti. CNR-GNDCI, Linea 3. Rapporto annuale 1989, U.O. 3.22 235–254.

Carrara, A., Cardinali, M., Guzzetti, F., Reichenbach, P., 1995. GIS Technology in Mapping Landslide Hazard. Kluwer Academic Publishers, Dordrect, pp. 135–175.

Carrara, A., Guzzetti, F., Cardinali, M., Reichenbach, P., 1999. Use of GIS technology in the prediction and monitoring of landslide hazard. Natural Hazards 20, 117–135.

Chung, C., Fabbri, A., Van Westen, C.J., 1995. Multivariate regression analysis for landslide hazard zonation. In: Carrara, A., Guzzetti, F. (Eds.), Geographical Information Systems in Assessing Natural Hazard. Kluwer Academic Publishers, Dordrecht, The Netherlands, pp. 107–142.

Dai, C., Lee, C.F., 2002. Landslide characteristics and slope instability modeling using GIS, Lantau Island, Hong Kong. Geomorphology 42, 213–228.

DeGraff, J., Romesburg, H., 1980. In: Coates, D., Vitek, J. (Eds.), Regional Landslide-Susceptibility Assessment for Wildland Management: A Matrix Approach, pp. 401–414.

Ercanoglu, M., Gokceoglu, C., 2004. Use of fuzzy relations to produce landslide susceptibility map of a landslide prone area (West Black Sea Region, Turkey). Engineering Geology 5, 229–250.

ESRI, 1991. ARC-INFO 6.0 Reference Manual. Environmental System Research Institute Inc., Redlands, CA.

Fernandez, C.I., Del Castillo, T.F., Hamdouin, R., Chacon Montero, J., 1999. Verification of landslide susceptibility mapping: a case study. Earth Surface Processes and Landforms 24, 537–544.

Gorsevski, P.V., Gessler, P., Foltz, R.B., 2000. Spatial prediction of landslide hazard using logistic regression and GIS. Proc. 4th International Conference on Integrating GIS and Environmental Modelling (GIS/EM$): Problems, Prospect and Research Needs. Banff, Alberta, Canada.

Greco, R., 2004. Valutazione della suscettibilità ai fenomeni franosi mediante procedure innovative, unpublished PhD thesis, University of Calabria, Dep. of Earth Sciences, 328pp.

Guarascio, G., Silvano, S., Sorriso-Valvo, M., 2005. Regressione Logistica applicata alla valutazione della suscettibilità ai fenomeni

franosi della Fiumara La verde (Aspromonte, Calabria). Unpublished stage report, University of Padova, CNR-IRPI.

Guzzetti, F., 1993. Landslide hazard and risk by GIS-based mutivariate models. In: Reichenbach, P., Guzzetti, F., Carrara, A. (Eds.), Geographical Information Sistems in Assessing Natural Hazard-Abstract, CNR, Perugia, September 20–22, 1993, pp. 83–91.

Guzzetti, F., Cardinali, M., 1989. Digital elevation models for landslide susceptibility maps. Proc. 20th Annual Pittsburg Conference on Modelling and Simulation, Pittsburgh, U.S.A, pp. 1541–1544.

Guzzetti, F., Cardinali, M., Mark, R.K., 1987. Analisi statistico-brobabilistica sulla distribuzione dei fenomeni franosi nell'area di Gualdo Tadino. Umbria-Italia Centrale. Rapporto Interno CNR-IRPI, vol. 92, p. 20.

Guzzetti, F., Carrara, A., Cardinali, M., Reichenbach, P., 1999. Landslide hazard evaluation: a review of current techniques and their application in a multi-scale study, Central Italy. Geomorphology 31, 181–216.

Iwahashi, J., Watanabe, S., Furuya, T., 2003. Mean slope-angle frequency distribution and size frequency distribution of landslide masses in Higashikubiki area, Japan. Geomorphology 50, 349–364.

Lineback, M., Andrew, W., Aspinall, R., Custer, S., 2001. Assessing landslide potential using GIS, soil wetness modelling and topographic attributes, Payette River, Idaho. Geomorphology 37, 149–165.

Maharaj, R.J., 1993. Landslide processes and landslide susceptibility analysis from an upland watershed: a case study from St., Andrew, Jamaica, West Indies. Engineering Geology 34, 53–79.

Ohlmacher, G.C., Davis, J.C., 2003. Using multiple logistic regression and GIS technology to predict landslide hazard in northeast Kansas, USA. Engineering Geology 69, 331–343.

Ogniben, L., 1960. Nota illustrativa dello schema geologico della Sicilia nord-orientale. Rivista Mineraria Siciliana 64–65, 183–212.

Ordan, C., O'Connor, E., Marchant, A., Northmore, A., Greenbaum, D., McDonald, A., Kovacik, M., Ahmed, R., 2000. Rapid landslide susceptibility mapping using remote sensing and GIS modelling. Proc. 14th International Conference on Applied Geologic Remote Sensing, Las Vegas, pp. 113–120.

Reger, J.P., 1979. Discriminant analysis as possible tool in landslide investigations. Earth Surface Processes and Landforms 4, 267–273.

Reichenbach, P., Guzzetti, F., Carrara, A. (Eds.), 1993. Workshop on Geographical Information Systems in Assessing Natural Hazard. Villa la Colombella, Perugia, Italia, p. 140. Abstracts volume.

Sorriso-Valvo, M., 1979. Trench features on steep-sides ridges, Aspromonte, Calabria (Italy). Superficial Mass Movement in Mountain Regions. Polish-Italian Seminar, Poland, Szymbark.

Sorriso-Valvo, M., 1982. Landslide Map of the Buonamico Basin. F.U., Berlin.

Sorriso-Valvo, M., 1989. Influence of tectonics on spatial distribution of mass movements: Calabrian case studies. Proc. 28th Int. Geological Congress, Washington, D.C. USA, July 9–19, pp. 3–156.

Sorriso-Valvo, M., 1993. The geomorphology of Calabria, a sketch. Geografia Fisica e Dinamica Quaternaria 16, 75–80.

Sorriso-Valvo, M., 2002. Landslides: from inventory to risk. Proc. 1st European Conference on Landslides, Prague, Czech Republic. A.A. Balkema Publishers.

Sorriso-Valvo, M., Gullà, G., 1996a. Block slide. In: Dikau, R., Brunsden, D., Schrott, L., Ibsen, M.L. (Eds.), Landslide Recognition: Identification, Movement and Causes. IAG Publication, vol. 5, pp. 85–96.

Sorriso-Valvo, M., Tansi, c., 1996b. Attività franosa in relazione all' attività tettonica recente nella media Valle del Fiume Crati. Il Quaternario 9, 345–352.

Suzen, M.L., Doyuran, V., 2004. Data driven bivariate landslide susceptibility assessment using geographical information systems: a method and application to Asarsuyu catchment, Turkey. Engineering Geology 71, 303–321.

Van Westen, C.J., 1992. Scale related GIS techniques in the analysis of landslide hazard. Proc. 1st Int. Symp. on Remote Sensing and GIS for Natural Risk Studies, Bogota.

Varnes, D.J., 1978. Slope movement types and processes. In Schuster, R.L., Krizek, R.J. (Eds.), Landslides. Analysis and Control. Transp. Res. Board Special Publication, 176, Nat. Acad. Sc., 11–33, 1 pl.

Versace, P., Ferrari, E., Gabriele, S., Rossi, F., 1989. Valutazione delle piene in Calabria, CNR-IRPI. Geodata 30.